ISSN 1062-8738, Bulletin of the Russian Academy of Sciences: Physics, 2023, Vol. 87, Suppl. 1, pp. S36–S40. © Pleiades Publishing, Ltd., 2023.

$La_{0.5}Sr_{0.5}FeO_{3-\gamma}$ Ferrite Studied by Raman Spectroscopy

K. A. Gavrilicheva[a], * (ORCID: 0009-0000-1403-7144), O. I. Barkalov[a], and V. D. Sedykh[a]

[a] *Osipyan Institute of Solid-State Physics, Russian Academy of Sciences, Chernogolovka, Moscow Region, 142432 Russia*

**e-mail: xenia.gavrilicheva@issp.ac.ru*

Received September 14, 2023; revised October 2, 2023; accepted October 9, 2023

Abstract—Transformations of polycrystalline $La_{0.5}Sr_{0.5}FeO_{3-\gamma}$ ferrites subjected to vacuum annealing in the temperature range of 400–650°C were studied by Raman spectroscopy at ambient conditions. It was shown that the homogeneity of the sample and its local ordering depended on the vacuum annealing temperature. An increase in the vacuum annealing temperature resulted in a gradual loss of oxygen and a transition of all iron ions to the oxidation state Fe^{3+}. These ferrites demonstrated a shift of the whole Raman spectra (including two-magnon modes) to higher frequencies with increasing Sr content of $0 < x < 0.5$. The possible reasons for the observed effects are discussed.

Keywords: ferrites, perovskites, Raman spectroscopy

DOI: 10.1134/S1062873823704373

INTRODUCTION

Ferrites with a perovskite-type structure ($\mathbf{R}_{1-x}\mathbf{A}_x FeO_{3-\gamma}$, where **R** is the rare-earth element, **A** is Ca, Sr, or Ba) have unique electrical, magnetic, and catalytic properties that make them suitable for many applications. They are used as cathode materials of solid oxide fuel cells due to their high ionic conductivity [1–3] and in catalytic reactions to decompose combustion products [4, 5]. Moreover, some compounds have antiferromagnetic properties, which enable their use as materials for magnetic memory devices. The $LaFeO_3$ and $SrFeO_{2.5}$ ferrites are antiferromagnets at room temperature. Their Neel temperatures are $T_N \sim 750$ K [6, 7] and ~690 K [8], respectively.

In the substituted $La_{1-x}Sr_xFeO_{3-\gamma}$ lanthanum ferrite, a gradual loss of oxygen and an increase in the number of oxygen vacancies occurred with an increase in the vacuum annealing temperature. It was shown in our previous papers that this process was accompanied by a change in the oxidation state of iron ions from a mixed Fe^{3+}/Fe^{4+} state to a pure Fe^{3+} one [9–12]. The composition of these ferrites, with Fe^{3+} ions, can be described by the general formula $La_{1-x}Sr_xFeO_{3-x/2}$. In the compositions with Sr content of $0 < x < 0.5$, these ferrites have an orthorhombic structure, and for the $La_{0.5}Sr_{0.5}FeO_{2.75}$ ferrite a cubic structure ($Pm\bar{3}m$ space group) for a metal sublattice is attained [11].

The $SrFeO_3$ ferrite with a high-symmetry cubic $Pm\bar{3}m$ structure does not have Raman active modes. In the orthorhombic $LaFeO_3$, Fe^{3+} ions have a distorted octahedral environment FeO_6, therefore, this lattice gives Raman active modes. In [13], rare-earth orthoferrites were studied by Raman spectroscopy, and the ab initio calculations performed allowed for a reliable mode assignment of the peaks in the experimental spectra. According to [11], in the $La_{0.5}Sr_{0.5}FeO_{2.75}$ ferrite obtained by vacuum annealing at 650°C, the metallic sublattice is well described by a cubic structure with $a = 3.914(1)$ Å ($Pm\bar{3}m$ space group). Nevertheless, this oxygen-deficient ferrite has a Raman spectrum composed of a series of broad peaks. As was demonstrated in [9–12] for La/Sr ferrites, in the Raman spectra there were low–frequency phonon modes (below 1000 cm^{-1}). In addition, there was a high-frequency broad band (above 1000 cm^{-1}) associated with two-magnon scattering [14–16].

In our recent publications [9–11] we studied by means of X-ray diffraction, Mössbauer spectroscopy and, in part only, by Raman spectroscopy structural changes, evolution of the Fe ions oxidation state and their local oxygen environment in the course of vacuum annealing. This was done for the samples with the fixed La/Sr ratio.

In the present work, the whole set of the Raman spectroscopy data is reported. The Raman spectra of La/Sr ferrites with Fe ions in the Fe^{3+} oxidation state (i.e. the lowest oxygen content for a given La/Sr ratio) were analyzed for the entire composition range from $LaFeO_3$ to $SrFeO_{2.5}$ ferrite. The effect of strontium substitution on the evolution of the ferrite Raman spectra was analyzed. We studied in detail transformations of the substituted $La_{0.5}Sr_{0.5}FeO_{3-\gamma}$ ferrite subjected to vacuum annealing as the equally distant one from the edges in terms of La/Sr composition.

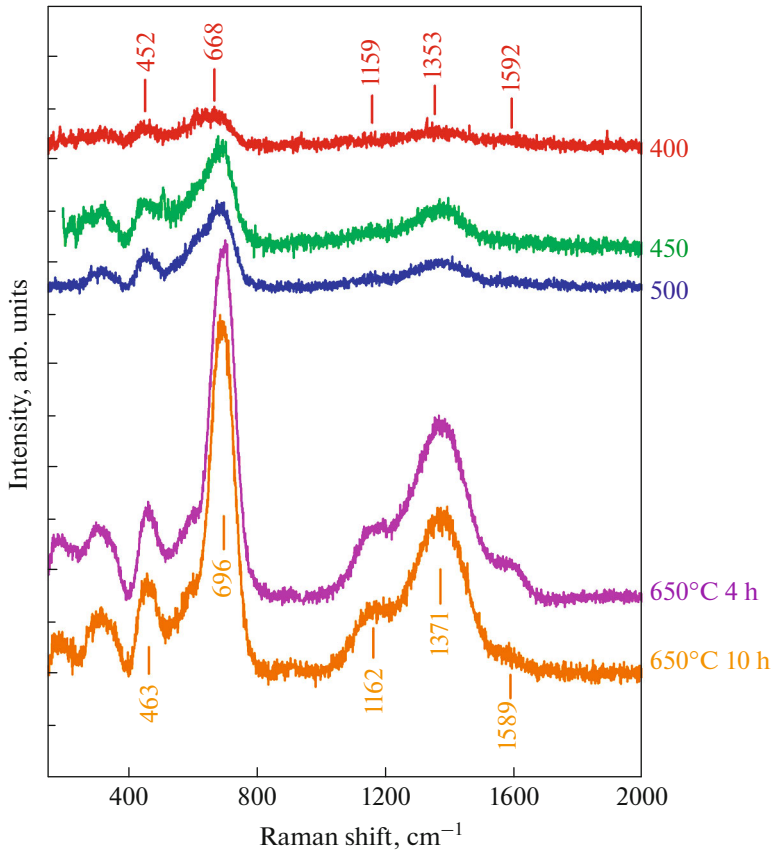

Fig. 1. Raman spectra of the $La_{0.5}Sr_{0.5}FeO_{3-\gamma}$ ferrites. The samples were annealed in vacuum (10^{-3} Torr, 4 h) at temperatures within the range of 400–650°C. The lowest spectrum corresponds to the sample annealed at 650°C for 10 h. All spectra were acquired with the same laser excitation power, exposure time, and number of accumulations. The featureless smooth background was subtracted manually from the spectra.

EXPERIMENTAL

Polycrystalline $La_{0.5}Sr_{0.5}FeO_{3-\gamma}$ sample was synthesized in the air by a glycine-nitrate combustion method at 1100°C for 20 h using La, Sr, and Fe nitrates in a stoichiometric proportion and glycine as starting reagents. The details of the preparation procedure were described in [9]. After the synthesis, the sample and the furnace were cooled down slowly to room temperature. Portions of as-prepared $La_{0.5}Sr_{0.5}FeO_{2.86}$ were annealed in vacuum (10^{-3} Torr) at 400–650°C for 4 h to decrease oxygen concentration in the lattice. The last sample of this series was annealed at 650°C for 10 h to make certain that the state finally stabilized.

The Raman spectra were recorded with a Princeton Instruments HRS 500 spectrometer equipped with a liquid nitrogen-cooled charge-coupled device detector and a grating of 1200 grooves/mm. The samples were irradiated in a back-scattering geometry at room temperature with a 532 nm DPSS laser. The laser power at the sample was ~5 mW. A 20x Plan Apo Mitutoyo objective was used to focus the excitation laser line and collect scattered light. The beam spot on the sample surface was about 3 μm in diameter. The razor edge (Semrock) and holographic Notch filters (Tydex) were used for laser line discrimination. The Raman spectra were acquired above ~150 cm^{-1}. The spectral resolution in the studied spectral range was ≈1 cm^{-1}. The Raman spectrometer was calibrated using Ne spectral lines with an uncertainty of ±1 cm^{-1}.

The phase composition, crystalline structure, and local atomic order of Fe ions were characterized by powder X-ray diffraction and Mössbauer spectroscopy. The results of these studies and details of the experimental methods were reported in [11].

RESULTS AND DISCUSSION

For all vacuum annealing temperatures, the number of Raman spectra from different points on the sample surfaces was acquired. Representative spectra are shown in Fig. 1. An increase in the annealing temperature leads to a decrease in the linewidth of the peaks and a profound increase in their intensity. This effect indicates the improvement of the ferrite crystalline structure. Longer annealing time of 10 h at 650°C does not result in any conspicuous change in the

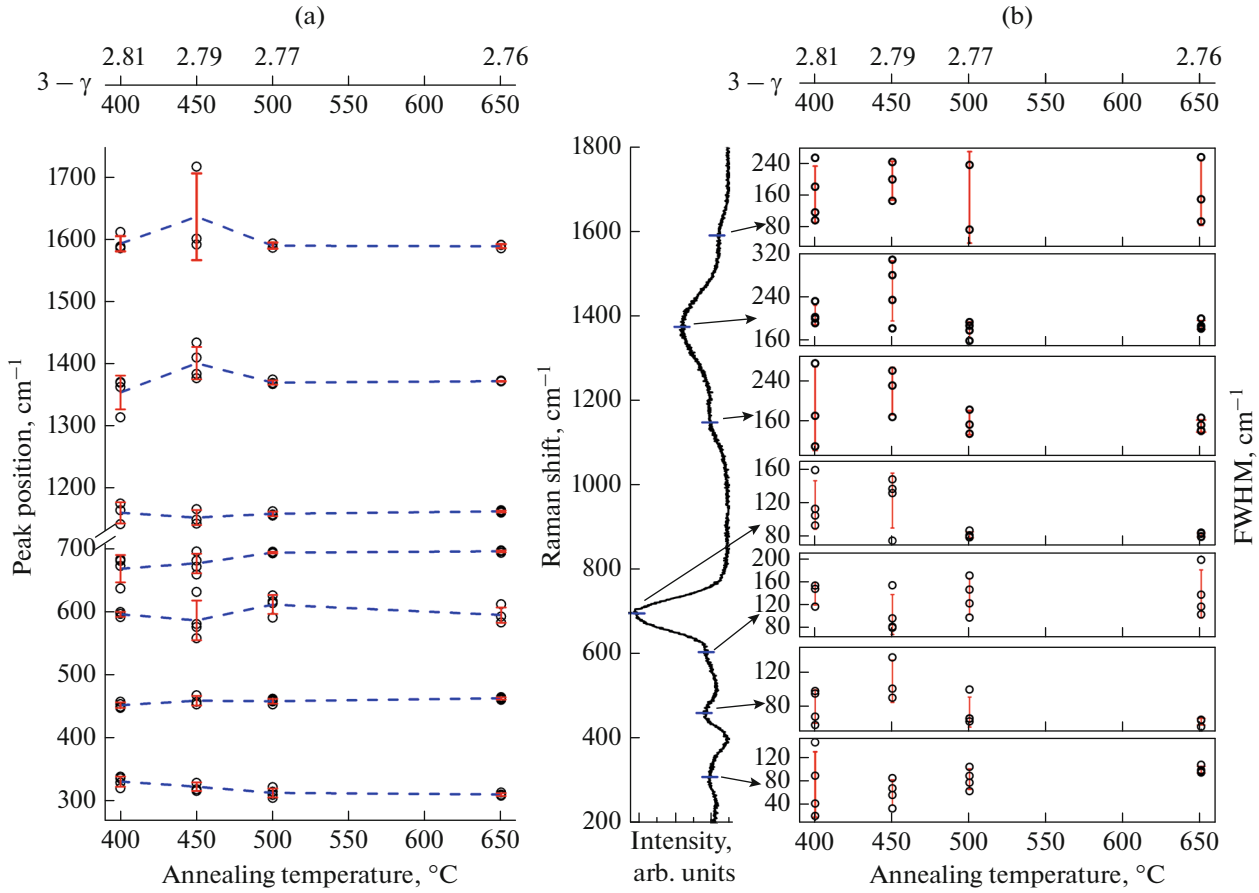

Fig. 2. Dependence of (a) the peak positions and (b) the full width at the half maximum on the annealing temperature (bottom scale) and oxygen content in the $La_{0.5}Sr_{0.5}FeO_{3-\gamma}$ samples (upper scale). Open circles denote the values obtained for different points of the sample. Red error bars indicate a standard deviation from the average of the point spread. Dash lines drawn through the mean values are the guides for the eye.

Raman spectrum (compare the two lowest spectra of the sample, Fig. 1).

An increase in the annealing temperature leads to a decrease in the oxygen content in ferrites. Peak positions and the full width at the half maximum (FWHM) of the Raman active modes monitored within the 150–2000 cm^{-1} interval are plotted as a function of the annealing temperature and oxygen content (the parameter $3-\gamma$) in Fig. 2. The oxygen contents in all samples were determined using the Mössbauer spectroscopy data from [11]. The applicability of this method for the estimation of oxygen content was demonstrated in [12] for $SrFeO_{3-\delta}$ ferrites.

The frequency range of the Raman spectra can be divided into two intervals. The low–frequency bands (below 1000 cm^{-1}) correspond to the phonon–like vibrations, and the high–frequency ones (above 1000 cm^{-1}) are probably due to magnons of the ferrite antiferromagnetic sublattices since, according to the calculations of Weber et al. [13], no phonon–like vibrations in the parent $LaFeO_3$ ferrite have frequencies higher than 650 cm^{-1}.

Figures 2a and 2b show that the spread of the peak positions over the sample points, as well as corresponding FWHM, decreases substantially with an increase in the annealing temperature. Above 500°C, a homogeneous state and composition uniformity are observed.

The dependence of the formula unit volume of $La_{1-x}Sr_xFeO_{3-x/2}$ ferrites on the strontium content for $x = 0$–0.5 is presented in Fig. 3. The structural data available in the literature [17–19] and from our recent publications [10, 11] were used to calculate the specific volume of the ferrites. This dependence is close to a linear one. The substitution of La^{3+} with Sr^{2+} leads to a relative volume decrease of ~1.2% and, hence, a decrease in the Fe–O bond length. This is the reason for the hardening of phonon modes.

The ab initio calculations performed in [13] for $LaFeO_3$ allowed for a reliable vibration mode assignment of the experimental peaks. The peaks in low-fre-

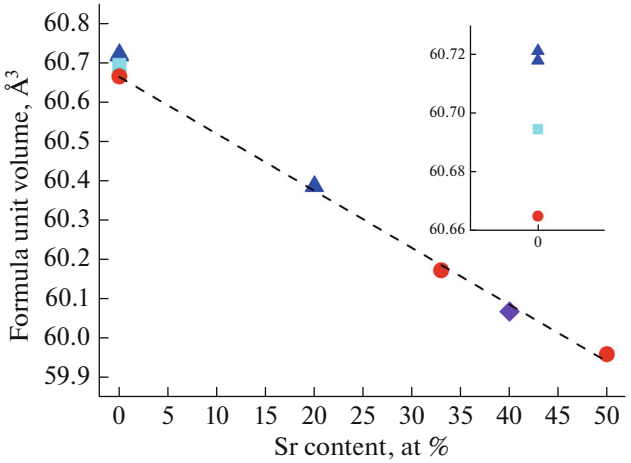

Fig. 3. Dependence of the formula unit volume on the strontium content in the $La_{1-x}Sr_xFeO_{3-x/2}$ ferrites ($x \leq 0.5$). Triangles note the data from [17], a square—from [19], a rhomb—from [18], and circles—from [10, 11]. A dashed line is the approximating linear function of points (for $x = 0$, the point marked with the circle was taken).

quency range correspond to the following Fe–O vibration modes: two-centered (Fe–O), three-centered (O–Fe–O), and multicentered (FeO_6 – squeezing, rotation, and breathing). The Raman spectra of the substituted $La_{0.67}Sr_{0.33}FeO_{2.84}$ and $La_{0.5}Sr_{0.5}FeO_{2.76}$ ferrites presented in Fig. 4 appear as a set of broad bands in contrast to pure $LaFeO_3$ and $SrFeO_{2.5}$. The peak broadening is due to the existence of oxygen vacancies in the crystal structure of these substituted ferrites. The frequency intervals and relative intensities of the substituted ferrites spectra resemble the spectrum of the pure $LaFeO_3$ ferrite. With increasing of strontium content, both phonon and magnon bands shift to higher frequencies. This effect might be due to the shortening of Fe–O bonds.

Further substitution of La with Sr, $x > 0.5$, does not lead to a noticeable shift of the Raman spectra to higher frequencies (compare the spectra of $La_{0.67}Sr_{0.33}FeO_{2.84}$ and $La_{0.5}Sr_{0.5}FeO_{2.76}$ with that of $SrFeO_{2.5}$), which apparently results from phase transformation in the strontium-rich ferrites and the emergence of FeO_4 tetrahedra [20, 21].

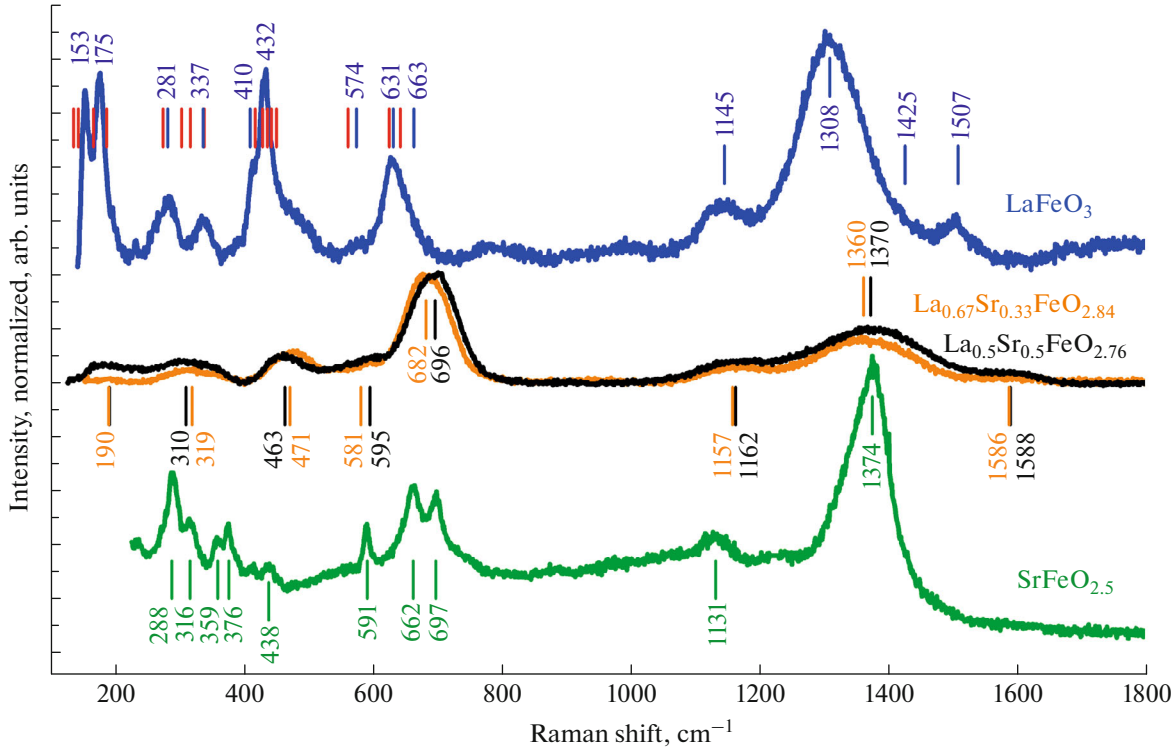

Fig. 4. Raman spectra of the $La_{1-x}Sr_xFeO_{3-\gamma}$ ferrites with Fe ions in a Fe^{3+} oxidation state. The intensities of the spectra were normalized to the intensity of the peak in the range of 600–700 cm^{-1}. Black spectrum was presented for $La_{0.5}Sr_{0.5}FeO_{2.76}$ annealed at 650°C for 4 h. The spectra for $LaFeO_3$ and $La_{0.67}Sr_{0.33}FeO_{2.84}$ were taken from [10], and for $SrFeO_{2.5}$—from [12]. Red vertical bars denote the experimental positions of $LaFeO_3$ peaks presented in Table II of [13]. The exact sample compositions are given on the right side. (For interpretation of the references to color in this figure legend, the reader is referred to the Web version of this article.)

CONCLUSIONS

Summarizing the results obtained, we come to the following conclusions.

An increase in the vacuum annealing temperature in the $La_{0.5}Sr_{0.5}FeO_{3-\gamma}$ ferrite leads to improvement in the crystal structure and noticeable homogenization of the sample.

For the substituted $La_{1-x}Sr_xFeO_{3-x/2}$ ferrites with Sr content of $0 < x < 0.5$ and Fe ions in the oxidation state Fe^{3+}, a perceptible shift of the whole Raman spectra to higher frequencies is observed. It might be due to a decrease in the specific volume and a corresponding decrease in the Fe–O bond lengths.

ACKNOWLEDGMENTS

The authors wish to acknowledge using the micro-Raman optical system of the Research Facility Center in the Osipyan Institute of Solid State Physics, Russian Academy of Sciences, for the data acquisition.

FUNDING

This work was carried out within the framework of the state task of the Osipyan Institute of Solid State Physics, Russian Academy of Sciences.

CONFLICT OF INTEREST

The authors declare that they have no conflicts of interest.

REFERENCES

1. Shaula, A., Pivak, Y., Waerenborgh, J., Gaczynski, P., Yaremchenko, A., and Kharton, V., *Solid State Ionics*, 2006, vol. 177, p. 2923.
2. Patrakeev, M.V., Bahteeva, J.A., Mitberg, E.B., Leonidov, I.A., Kozhevnikov, V.L., and Poeppelmeier, K.R., *J. Solid State Chem.*, 2003, vol. 172, p. 219.
3. Shin, Y., Doh, K.-Y., Kim, S.H., Lee, J.H., Bae, H., Song, S.-J., and Lee, D., *J. Mater. Chem. A*, 2020, vol. 8, p. 4784.
4. Wei, Z.-X., Xu, Y.-Q., Liu, H.-Y., and Hu, C.-W., *J. Hazard. Mater.*, 2009, vol. 165, p. 1056.
5. Tijare, S.N., Joshi, M.V., Padole, P.S., Mangrulkar, P.A., Rayalu, S.S., and Labhsetwar, N.K., *Int. J. Hydrogen Energy*, 2012, vol. 37, p. 10451.
6. Goodenough, J.B., *Magnetism and the Chemical Bond*, New York: Wiley, 1963, vol. 1.
7. Boekema, C., Jonker, P.C., Filoti, G., van der Woude, F., and Sawatzky, G.A., *Hyperfine Interact.*, 1979, vol. 7, p. 45.
8. Schmidt, M. and Campbell, S.J., *J. Solid State Chem.*, 2001, vol. 156, p. 292.
9. Sedykh, V.D., Rybchenko, O.G., Nekrasov, A.N., Koneva, I.E., and Kulakov, V.I., *Phys. Solid State*, 2019, vol. 61, p. 1099.
10. Sedykh, V., Rybchenko, O., Rusakov, V., Zaitsev, S., Barkalov, O., Postnova, E., Gubaidulina, T., Pchelina, D., and Kulakov, V., *J. Phys. Chem. Solids*, 2022, vol. 171, p. 111001.
11. Sedykh, V., Rusakov, V., Rybchenko, O., Gapochka, A., Gavrilicheva, K., Barkalov, O., Zaitsev, S., and Kulakov, V., *Ceram. Int.*, 2023, vol. 49, p. 25640.
12. Barkalov, O.I., Zaitsev, S.V., and Sedykh, V.D., *Solid State Commun.*, 2022, vol. 354, p. 114912.
13. Weber, M.C., Guennou, M., Zhao, H.J., Íñiguez, J., Vilarinho, R., Almeida, A., Moreira, J.A., and Kreisel, J., *Phys. Rev. B*, 2016, vol. 94, p. 214103.
14. Anokhin, A.S., Razumnaya, A.G., Torgashev, V.I., Trotsenko, V.G., Yuzyuk, Yu.I., Bush, A.A., Shkuratov, V.Ya., Gorshunov, B.P., Zhukova, E.S., Kadyrov, L.S., and Komandin, G.A., *Phys. Solid State*, 2013, vol. 55, p. 1417.
15. Andreasson, J., Holmlund, J., Knee, C.S., Käll, M., Börjesson, L., Naler, S., Bäckström, J., Rübhausen, M., Azad, A.K., and Eriksson, S.-G., *Phys. Rev. B*, 2007, vol. 75, p. 104302.
16. Manzoor, S., Husain, S., and V. Raghavendra Reddy, *Appl. Phys. Lett.*, 2018, vol. 113, p. 072901.
17. Dann, S.E., Currie, D.B., Weller, M.T., Thomas, M.F., and Al-Rawwas, A.D., *J. Solid State Chem.*, 1994, vol. 109, p. 134.
18. Yang, J.B., Yelon, W.B., James, W.J., Chu, Z., Kornecki, M., Xie, Y.X., Zhou, X.D., Anderson, H.U., Joshi, A.G., and Malik, S.K., *Phys. Rev. B*, 2002, vol. 66, p. 184415.
19. Selbach, S.M., Tolchard, J.R., Fossdal, A., and Grande, T., *J. Solid State Chem.*, 2012, vol. 196, p. 249.
20. Sedykh, V.D., Rybchenko, O.G., Barkovsky, N.V., Ivanov, A.I., and Kulakov, V., *Fiz. Tverd. Tela*, 2021, vol. 63, p. 1648.
21. Auckett, J.E., Studer, A.J., Sharma, N., and Ling, C.D., *Solid State Ionics*, 2012, vol. 225, p. 432.

Publisher's Note. Pleiades Publishing remains neutral with regard to jurisdictional claims in published maps and institutional affiliations.